Clim Dyn (2012) 39:313–327
DOI 10.1007/s00382-011-1188-9

Interdecadal changes in the storm track activity over the North Pacific and North Atlantic

Sun-Seon Lee · June-Yi Lee · Bin Wang · Kyung-Ja Ha · Ki-Young Heo · Fei-Fei Jin · David M. Straus · Jagadish Shukla

Received: 3 March 2011 / Accepted: 3 September 2011 / Published online: 17 September 2011
© Springer-Verlag 2011

Abstract Analysis of NCEP-NCAR I reanalysis data of 1948–2009 and ECMWF ERA-40 reanalysis data of 1958–2001 reveals several significant interdecadal changes in the storm track activity and mean flow-transient eddy interaction in the extratropics of Northern Hemisphere. First, the most remarkable transition in the North Pacific storm track (PST) and the North Atlantic storm track (AST) activities during the boreal cold season (from November to March) occurred around early-to-mid 1970s with the characteristics of global intensification that has been noticed in previous studies. Second, the PST activity in midwinter underwent decadal change from a weak regime in the early 1980s to a strong regime in the late 1980s. Third, during recent decade, the PST intensity has been enhanced in early spring whereas the AST intensity has been weakened in midwinter. Finally, interdecadal change has been also noted in the relationship between the PST and AST activities and between the storm track activity and climate indices. The variability of storm track activity is well correlated with the Pacific Decadal Oscillation and North Atlantic Oscillation prior to the early 1980s, but this relationship has disappeared afterward and a significant linkage between the PST and AST activity has also been decoupled. For a better understanding of the mid-1970s' shift in storm track activity and mean flow-transient eddy interaction, further investigation is made by analyzing local barotropic and baroclinic energetics. The intensification of global storm track activity after the mid-1970s is mainly associated with the enhancement of mean meridional temperature gradient resulting in favorable condition for baroclinic eddy growth. Consistent with the change in storm track activity, the baroclinic energy conversion is significantly increased in the North Pacific and North Atlantic. The intensification of the PST and AST activity, in turn, helps to reinforce the changes in the middle-to-upper tropospheric circulation but acts to interfere with the changes in the low-tropospheric temperature field.

Keywords Storm track · Interdecadal shift · Climate change · Barotropic and baroclinic energetics · Mean flow-eddy interaction

S.-S. Lee · K.-J. Ha (✉) · K.-Y. Heo
Division of Earth Environmental System, Pusan National University, Busan, Korea
e-mail: kjha@pusan.ac.kr

J.-Y. Lee · B. Wang · F.-F. Jin
Department of Meteorology and International Pacific Research Center, University of Hawaii, Honolulu, Hawaii

D. M. Straus · J. Shukla
George Mason University, Fairfax, VA, USA

D. M. Straus · J. Shukla
Center for Ocean-Land-Atmosphere Studies, Calverton, MD, USA

1 Introduction

Given the fact that storm track activity is intimately linked to weather and short-term climate variability over the extratropics of the Northern Hemisphere (NH) during the cold season, changes in its intensity and location have a significant climate impact (Blackmon 1976; Lau 1988; Chang et al. 2002). Changes in storm track activity lead to not only global circulation changes through vertical and horizontal exchange of heat, water vapor, and momentum (Jin 2010; Kug et al. 2010) but also significant changes in the hydrological cycle through anomalous evaporation from the warm ocean surface and precipitation (Nakamura

et al. 2002). Understanding of interdecadal changes in storm track activity in the past may give a hint of how a future mean state change will modify the storm track's behavior and how its change, in turn, will have an effect on the mean state.

Significant interdecadal changes of the NH storm track activity have been seen during the early-to-mid 1970s over the North Pacific and North Atlantic (Trenberth and Hurell 1994; Chang and Fu 2002, 2003; Harnik and Chang 2003) and during the late 1980s and early 1990s over the North Pacific (Chang and Fu 2002; Nakamura et al. 2002; Zhang et al. 2007). The former is likely to be related to the remarkable interdecadal change after the mid-1970s in the low-frequency component of the background circulation and SST (Trenberth 1990; Trenberth and Hurrell 1994; Latif and Barnett 1994 and many others). Trenberth and Hurrell (1994) suggested that the interdecadal change was accompanied by a southward shift in the Pacific storm track (PST) activity which, in turn, helped to reinforce and maintain the anomalous upper-tropospheric atmospheric circulation. It was further shown that a significant transition from a weak to a strong storm track regime during early-to-mid 1970s is evident over not only the North Pacific and but also the North Atlantic in the reanalysis data (Chang and Fu 2002) and radiosonde data (Harnik and Chang 2003). The latter, on the other hand, is characterized by the enhanced PST activity in midwinter along with the weakening of the east Asian winter monsoon and the Aleutian low since the late 1980s (Nakamura et al. 2002). Zhang et al. (2007) suggested that the decadal intensification of the PST activity may be related with increase of deep convective clouds over the Pacific due to the aerosol effect from the increase of Asian pollution outflow.

In the meantime, there is considerable interannual-to-interdecadal variability of storm track activity driven by tropical heating, e.g. El Niño-Southern Oscillation (ENSO) (e.g. Straus and Shukla 1997; Zhu and Sun 1999; Zhang and Held 1999; Chang et al. 2002; Eichler and Higgins 2006) or linked with extratropical teleconnection patterns, such as the Arctic Oscillation (AO), North Atlantic Oscillation (NAO), and Pacific/North American (PNA) pattern (e.g. Rivière and Orlanski 2007; Nie et al. 2008; Pinto et al. 2011). During El Niño years, the PST shifts considerably eastward and southward and its intensity increases substantially (Zhu and Sun 1999). During winters with a strong positive AO anomaly, the Atlantic storm track (AST) activity intensifies significantly and shifts northward while the PST activity extends westward (Nie et al. 2008). In the positive phase of the NAO, the AST intensity increases (Rivière and Orlanski 2007). Pinto et al. (2011) showed a poleward shift of PST in the negative PNA phase based on a multi-century coupled global circulation model (CGCM) simulation. Previous studies pointed out the storm track feedback forcing on the Icelandic and Aleutian lows, which are closely related to the NAO and PNA (Honda et al. 2001, 2005; Honda and Nakamura 2001). The PST and AST activity contributes to the development and maintenance of the Icelandic and Aleutian lows.

Furthermore, the location of storm tracks is also related to the stratospheric circulation which controls the correlation between the North Pacific and the North Atlantic pressure patterns (Castanheira and Graf 2003). During weak polar vortex regimes, a significant southward displacement of storm track is found over the Atlantic sector (Baldwin and Dunkerton 2001).

This study revisits the interdecadal change of storm track activity after the mid-1970s in order to better understand how the interdecadal change of mean state during this period affected the interdecadal shift of storm track activity and how this change, in turn, played a role in the mean state change. The approach to depict the interdecadal changes of storm track activity in this study is similar as the one shown in Chang and Fu (2002) but particular attention is paid to the change in mean flow-eddy interaction by analyzing local energetics and eddy feedback to mean flow and important factors responsible for the change. In addition, we investigate characteristics of interdecadal changes of storm track activity during recent decades. Section 2 introduces the observed data and analysis methods to depict changes in storm track activity and mean flow-eddy interaction. In Sect. 3, the dominant mode of storm track variability is investigated along with jet stream variability. The changes in relationship between the storm track activity and climate indices are also examined. Section 4 explores the role of eddy feedback on mean state change by analyzing local energetics and important factors responsible for the mid-1970s' shift. Finally, a summary and discussion are provided in Sect. 5.

2 Data and analysis methods

In this study, the storm track activity is defined as the root mean square (RMS) of the 2–8 day band-pass filtered geopotential height at standard pressure levels (Blackmon et al. 1977; Mak and Deng 2007). The main results presented here are the analysis of the storm track activity at 300-hPa averaged from November to March (NDJFM) for 1948–2009. Empirical Orthogonal Function (EOF) analysis was used to identify the dominant mode of variability for the cold season storm track activity in the extratropics of NH (20°–70°N). This analysis identifies a pattern (EOF) and a principal component time series (PC) associated with each mode.

This study primarily uses the National Centers for Environmental Prediction-National Center for Atmospheric

Research (NCEP-NCAR) reanalysis data set (NCEP-1; Kalnay et al. 1996) covering 62 years from 1948 to 2009, including horizontal and vertical winds, temperature, geopotential height at standard pressure levels, and surface sensible and latent heat fluxes. To avoid problems arising from NCEP-1 data before the early 1960s, we also utilize the European Centre for Medium-Range Weather Forecasts (ECMWF) 40-years reanalysis (ERA-40) data from 1958 to 2001 (Uppala et al. 2005).

In order to explore whether the interdecadal variability of storm track activity has any linkage with circulation or ocean variability, the relationship with climate indices is examined. We obtained monthly AO, NAO, and PNA indices for 60 years of 1950–2009 from the Climate Prediction Center (CPC) website at http://www.cpc.noaa.gov/products/precip/CWlink/daily_ao_index/teleconnections.shtml. The monthly Niño 3.4 index was obtained from CPC website at http://www.cpc.ncep.noaa.gov/data/indices/sstoi.indices. We also used the monthly Pacific Decadal Oscillation (PDO) index from Joint Institute for the Study of the Atmosphere and Ocean (JISAO) website at http://jisao.washington.edu/pdo.

Both barotropic and baroclinic processes are important for the development of storm track activity (e.g. Lee 2000; Chang et al. 2002). The background flow, thermal gradient and eddy heat fluxes are closely related to baroclinic eddy growth (Lee et al. 2011). Changes of mean flow-eddy interaction are interpreted by analyzing barotropic and baroclinic energy conversion and eddy feedback to the mean field in the quasi-geostrophic framework that was based on the study by Cai et al. (2007). Detailed equations of the local energetics and eddy feedback are given in the "Appendix".

3 Interdecadal variability of storm track

3.1 The dominant mode of the variability

We first investigate the dominant EOF mode of the inter-annual-to-interdecadal variability of storm track activity during NDJFM for 62 years of 1948–2009 in the extratropics of NH using NCEP-1 and ERA-40 data. The first EOF (EOF1) mode features enhancement of storm track activity over most of the regions in the extratropics of NH including East Asia, the North Pacific, eastern North America, the North Atlantic, and western Europe after the mid-1970s (Figs. 1a, 2a), supporting Chang and Fu (2002)'s finding using the analysis of high-pass filtered DJF 300-hPa meridional velocity variance. The variability center over the North Pacific is located to the southeast of

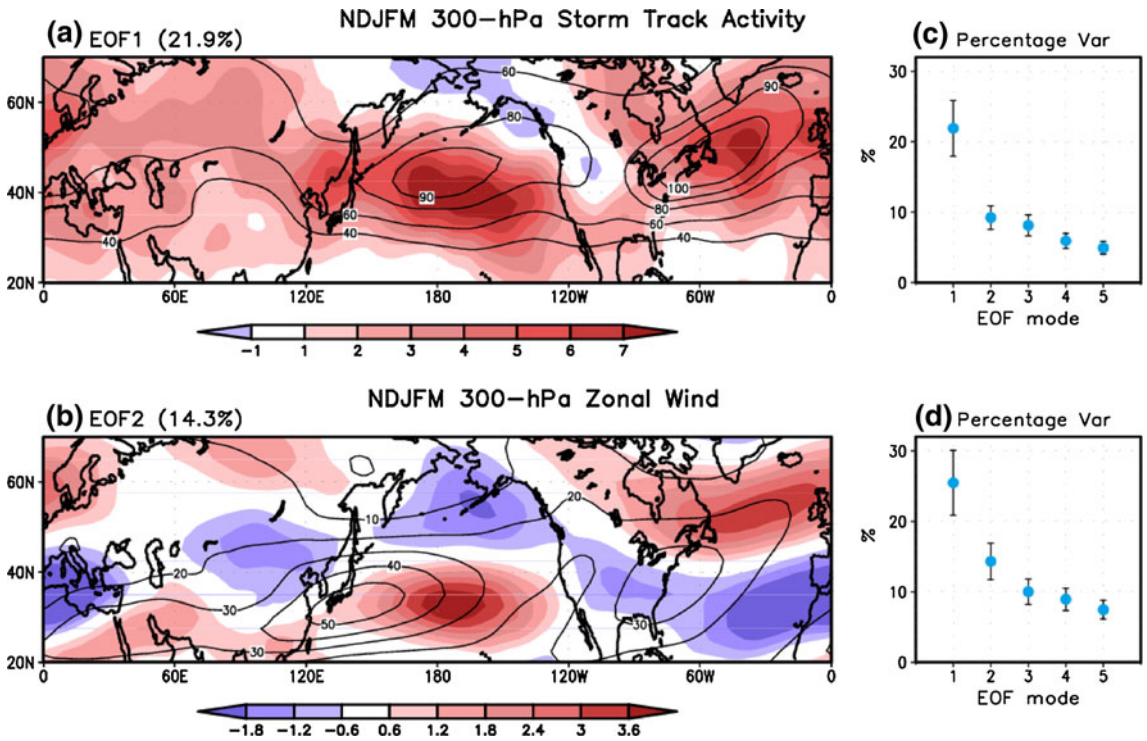

Fig. 1 Spatial patterns of **a** the first eigenvector (*shading*) of root-mean-square of the 2–8 day band-pass filtered 300-hPa geopotential height (m) superimposed by its climatology (contour) and **b** the second eigenvector of 300-hPa zonal wind (m s^{-1}) superimposed by its climatology using NCEP-1 reanalysis data. The percentage variances explained by the first five EOFs of **c** storm track activity and **d** 300-hPa zonal wind. The contour level of storm track activity in **a** is 40, 60, 80, 90, and 100 m and that of zonal wind in **b** is 20, 30, 40, and 50 m s^{-1}

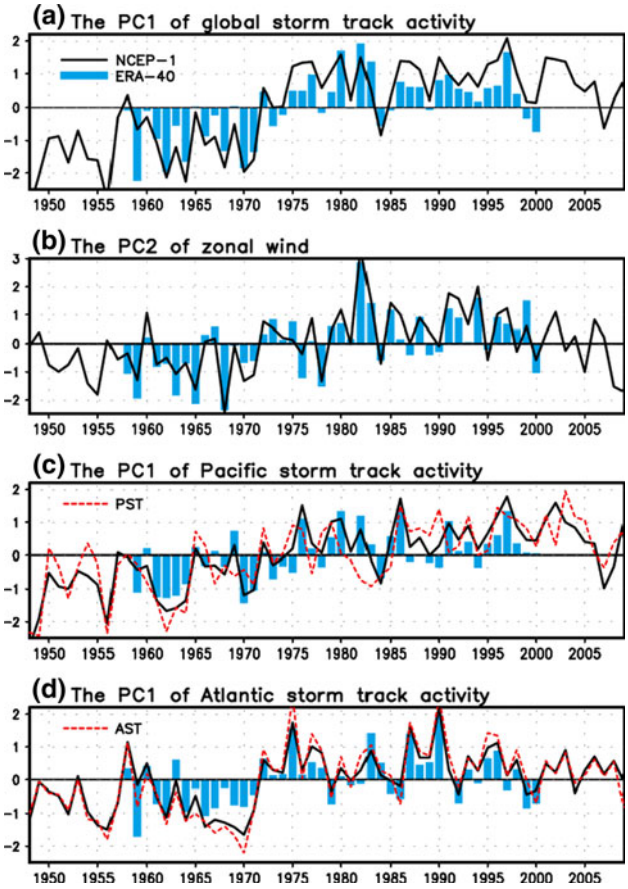

Fig. 2 **a** The first PC of 300-hPa storm track activity in the extratropics of NH (20–70°), **b** the second PC of 300-hPa zonal wind, **c** the first PC of 300-hPa storm track activity in the Pacific (20°–70°N, 120°–240°E), and **d** the first PC of 300-hPa storm track activity in the Atlantic (20°–70°N, 120°W–0°). The *red dashed line* in **c** and **d** indicates normalized time series of storm track activity averaged over the North Pacific (35°–60°N, 150°–220°E) and the North Atlantic (37.5°–62.5°N, 90°–20°W), respectively

the climatological PST peak position and that over the North Atlantic is located to downstream of the climatological AST activity peak (Fig. 1a). The EOF1 is statistically well separated from other higher modes (Fig. 1c) accounting for 21.9% of total variance and represents covariability between the PST and AST on both interannual and interdecadal time scale. The transition from weak to strong storm track activity regime during the mid-1970s is evident in the first principal component (PC1) from both NCEP-1 and ERA-40 (Fig. 2a). Furthermore, we also examine the dominant EOF mode for 2–8 day band-pass filtered 300-hPa meridional velocity variance for NDJFM from 1948 to 2009 and obtain quite comparable spatial pattern to that of geopotential height. The EOF1 of band-pass filtered 300-hPa meridional velocity variance accounts for 28.2% of total variance (not shown).

To find the change in jet stream related to the interdecadal variability of storm track activity, we perform EOF analysis of 300-hPa zonal wind during NDJFM for 62 years (Figs. 1b, 2b). The second PC (PC2) of 300-hPa zonal wind exhibits interdecadal variability (Fig. 2b). The correlation coefficient between the leading PC1 of storm track activity and the PC2 of zonal wind is 0.50 for 62 years which is statistically significant at 99% confidence level. This indicates that the EOF1 of global storm track intensity is related to the second EOF mode (EOF2) of seasonal mean zonal wind variability at 300-hPa. The EOF2 of zonal wind features eastward extension of the Pacific jet and northeastward extension of the Atlantic jet, accounting for 14.3% of total variance. Meanwhile, the PC1 of zonal wind is characterized by dominant interannual variability related to ENSO accounting for 26% of total variance (not shown).

Normalized time series of area mean storm track activity is also examined. The correlation coefficient between the PC1 of storm track activity in the Pacific [20°–70°N, 120°–240°E] and PST activity [35°–60°N, 150°–220°E] (between the PC1 of storm track activity in the Atlantic [20°–70°N, 120°W–0°] and AST activity [37.5°–62.5°N, 90°–20°W]) is 0.82 (0.96). It is evident that the transition from weak to strong regime is more remarkable in the North Atlantic than in the North Pacific. It is further noted that the AST activity shows a decreasing trend after the late 1980s whereas the PST activity does not have any trend during the period of interest (Fig. 2c, d). During recent decades, the PC2 of zonal wind tends to be decreasing (Fig. 2b) whereas the PC1 of storm track activity does not exhibit a clear trend (Fig. 2a). The mid-1970s' shift is also seen in the PC1 for band-pass filtered 300-hPa meridional velocity variance. The correlation coefficient between PC1 for band-pass filtered 300-hPa geopotential height and meridional velocity variance is 0.97.

Harnik and Chang (2003) suggested that there may be biases in the NCEP-NCAR reanalysis that spuriously exaggerated the mid-1970s' shift and long-term trend, particularly over the North Pacific. To alleviate the data problem, we compared results between NCEP-1 and ERA-40. The pattern correlation coefficient between the first eigenvector field from NCEP-1 and ERA-40 is 0.83 and the temporal correlation coefficient between the PC1 from NCEP-1 and ERA-40 is 0.89, suggesting that decadal changes in the EOF1 of storm track activity depicted by the reanalysis data may be significant.

Using observational data and GCM simulations, it has been noted that the interannual climate variation over the North Pacific is linked to that over the North Atlantic in the form of a seesaw-like oscillation between Aleutian and Icelandic lows (van Loon and Rogers 1978; Honda and Nakamura 2001; Raible et al. 2001; Orsolini et al. 2008) and its linkage has active and passive phases (Honda et al. 2005). Therefore, we examine the change in relationship

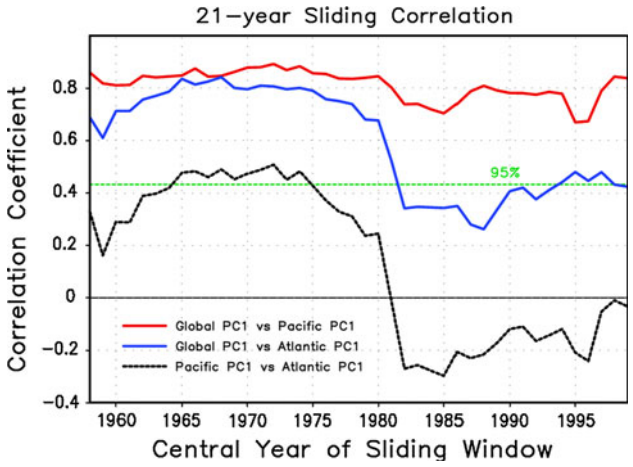

Fig. 3 Twenty-one-year sliding correlation coefficient between the PC1 of storm track activity in the extratropics of NH (global PC1) and the PC1 of storm track activity in the Pacific (Pacific PC1), between the global PC1 and the PC1 of storm track activity in the Atlantic (Atlantic PC1), and between the Pacific PC1 and Atlantic PC1 in NDJFM during 1948–2009. The *green horizontal line* shows the 95% confidence level

between interannual-to-interdecadal variability of storm track activity in the North Pacific and that in the North Atlantic (Fig. 3). The significant relationship between the PC1 of storm track activity in the extratropics of NH and in the North Pacific persists for 62 years, whereas storm track activity in the North Atlantic shows insignificant correlation with global storm track activity from 1980s to 1990s. It is interesting to note that the activities of PST and AST were closely connected each other during the period of 1965–1975 (as the central correlation year), but the activities of PST and AST have been decoupled since the early 1980s. However, it was found that the PST activity during winter is highly correlated to the AST activity during the period 1975/1976–1998/1999 when month-to-month variations are considered and the linkage between two storm tracks is weak during the period 1957/1958–1971/1972 (Chang 2004).

3.2 Interdecadal changes in annual cycle of storm track activity

As previous studies demonstrated (Nakamura 1992; Lee et al. 2011; and many others), the PST and the AST activities have a different annual cycle. The former shows distinctive double peaks in late fall and early spring with midwinter suppression regardless of the strongest baroclinicity. On the other hand, the latter shows a single maximum in January when the baroclinicity is the strongest over the North Atlantic. In this section, we investigate changes in the climatological annual cycle of the PST and AST intensity.

We first test significance of the mid-1970s' shift in the PC1 of global storm track intensity using the Lepage test (Yonetani and McCabe 1994). The test indicates that the shift occurring around 1970–1975 is highly significant at a confidence level of 99% with the Lepage statistic more than 10 (A brief summary is in the "Appendix"). There is no other significant shift in the test. Based on the PC1 of storm track activity in Fig. 2a, the strong storm track period (hereafter 'SP') is defined the 20-year period of 1975/1976–1994/1995 and the weak storm track period (hereafter 'WP') is defined the 20-year period of 1952/1953–1971/1972.

Figure 4a and b show interannual-to-interdecadal variability of the PST and AST intensity as a function of year and month. In addition, features of the annual cycle in PST and AST during SP, WP, and the most recent decade were compared and changes in annual cycle are presented in Fig. 4c and d. The PST activity exhibits three distinct changes in its annual cycle and interannual variability. First, after the mid-1970s, its intensity remarkably increased all through a year. Figure 4c clearly indicates that the amplitude of annual cycle was significantly enhanced from WP to SP. Second, the PST activity during midwinter was increased from the weak regime during the early 1980s (about 65–70 m) to the strong regime during the late 1980s (about 95–100 m) (Fig. 4a), which was shown in Nakamura et al. (2002). Lastly, the comparison of annual cycle between SP and the latest decade (1999–2009) in Fig. 4c suggests that the intensity during spring (March and April) increased in the latest decade while the intensity during fall (October and November) slightly decreased compared to that in SP. It is also shown that the second peak of its annual cycle was stronger than the first peak during the latest decade and WP whereas the first peak was stronger during SP.

The AST activity exhibits two distinct interdecadal changes (Fig. 4b). First, the amplitude of its annual cycle was significantly increased after the mid-1970s similar to the PST activity. In particular, the intensification from WP to SP is the largest in December and January (Fig. 4d). Second, since 1998/1999, the intensity during midwinter has been decreased while that during transition seasons has had no clear change. It is interesting to note that the intensity of the AST in January has been weakened during recent decade but that of the PST activity slightly enhanced.

3.3 Relationship with climate indices

To better understand the relationship between global circulation changes and storm track intensity, we investigate the relationship between the storm track intensity and climate indices for 60 years.

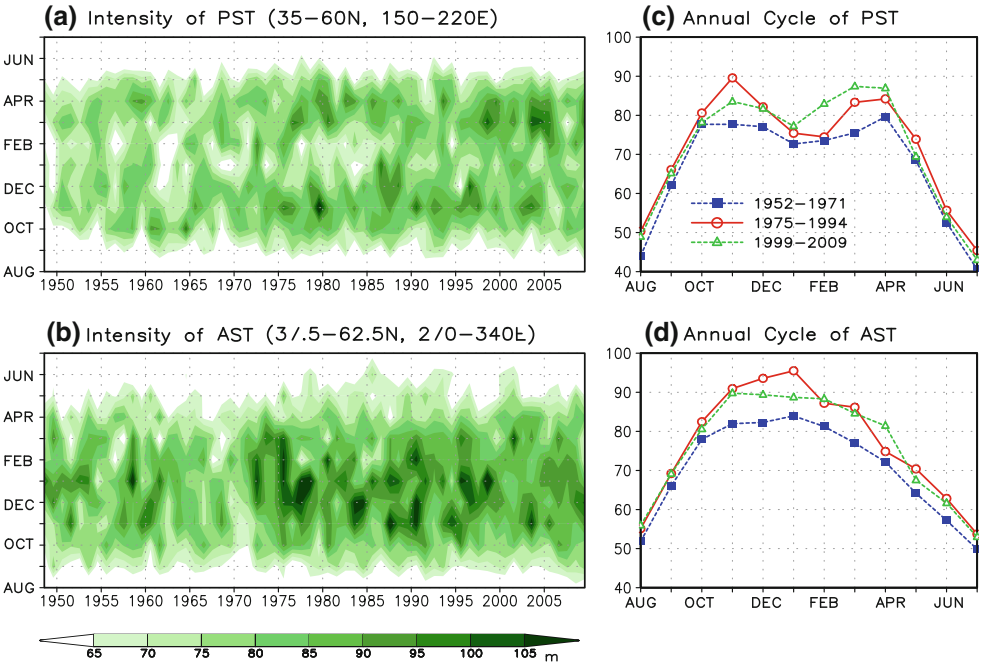

Fig. 4 Distribution of the **a** PST and **b** AST intensity (m) at 300-hPa with seasonal and interannual variabilities. The annual cycle of the **c** PST and **d** AST activity at 300-hPa during the 1952–1971, 1975–1994, and recent decade of 2000–2009

PC1 of global storm track intensity (ST PC1) well represents interannual-to-interdecadal variability of the PST and AST index with correlation coefficients of 0.73 and 0.75, respectively, for the 60 years and is well correlated with all climate indices used here except for AO shown in Table 1. As previous mentioned, the PC1 of global storm track intensity is also significantly linked with the PC2 of zonal wind. It is better correlated with the PDO index (correlation equals to 0.56) than other climate indices. While the global mode of storm track variability is well correlated with climate indices, the PST has a significant correlation coefficient just with the NAO index for 60 years. The AST activity is significantly related to the NAO and AO indices. This result is different from Chang and Fu (2002) showing that the PST activity is significantly correlated with the PDO while the AST activity with the NAO index. This is because the relationship between the storm track intensity and the climate indices has interdecadal changes shown in Fig. 5.

Figure 5 shows the 21-year sliding correlation between the storm track activity and climate indices. The relationships between storm track activity and climate indices exhibit interdecadal variations. The PC1 of storm track activity was highly correlated with the PDO and NAO during roughly 1960–1980 (as the central correlation year). However, those relationships have been much weakened since the early 1980s. Particularly, the relationships become nearly zero from mid-1980s to early 1990s. The correlation between the storm track activity and PDO has increased during recent the decade, whereas that between the storm track activity and NAO became negative. The changes of the sliding correlation between storm track activity and NAO are comparable to those between storm track activity and the AO. However, it is shown that PC1 of global storm track activity has no significant relationship with the AO for the entire period. The PC1 of storm track activity in the Atlantic was highly linked to the AO during 1960–1980, while the PC1 of storm track activity in the

Table 1 Temporal correlation coefficient between storm track activity and climate indices during 1950/1951–2009/2010

	ST PC1	ZW PC2	PST	AST	PDO	NAO	AO	PNA
ZW PC2	**0.55**	–	–	–	–	–		
PST	**0.73**	0.11	–	–	–	–		
AST	**0.75**	0.**41**	**0.48**	–	–	–		
PDO	**0.56**	0.**47**	0.25	0.20	–	–		
NAO	**0.47**	0.**71**	**0.38**	**0.48**	0.13	–		
AO	0.28	**0.54**	0.22	**0.46**	−0.18	**0.81**		
PNA	**0.48**	**0.48**	0.08	0.15	**0.76**	0.09	−0.16	
NINO3.4	**0.35**	0.26	0.14	0.04	**0.48**	−0.02	−0.15	**0.50**

Numbers in bold indicate significant correlation coefficients at 95% confidence level

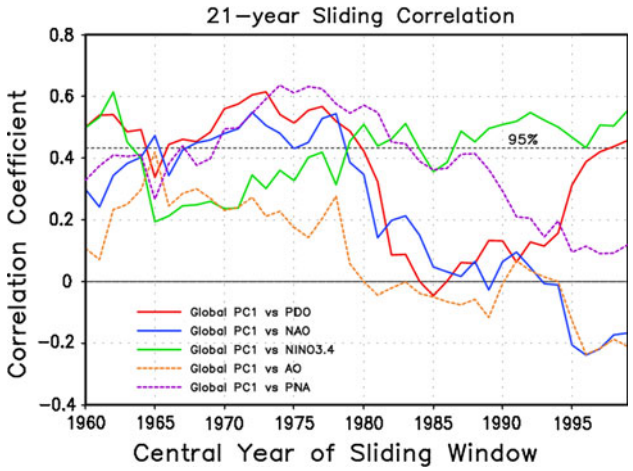

Fig. 5 Twenty-one-year sliding correlation coefficient between the PC1 of storm track activity over the extratropics of NH (global PC1) and climate indices

Pacific has no significant linkage with the AO (not shown). We found that storm track activity was strongly correlated to the PNA index during 1970–1980 and this significant correlation decreased continuously after the early 1980s. The relationship with Niño 3.4 shows an interdecadal change distinct from that with PDO or NAO, from a weak correlation regime during 1960–1980 to a strong correlation regime during 1980–2000. Causes of these interdecadal changes in the relationship between the storm track activity and climate indices addressed here deserve further investigation.

4 The mid-1970s' shift in mean flow-eddy interaction

This section is devoted to further examining the most striking interdecadal shift during mid-1970s' in storm tract activity and mean flow-eddy interaction. Particular attention is paid to the important factors responsible for the interdecadal change and eddy feedback to the mean flow by comparing storm track activity, mean status, and a local energetics between SP and WP periods.

4.1 Difference in storm track intensity

The storm track activity and jet intensity at 300-hPa averaged from November to March during the SP and the difference between the SP and WP using NCEP-1 are shown in Fig. 6. The composite patterns and difference between the two periods obtained from ECMWF ERA-40 are in highly agreement with those of NCEP-1 (not shown). The spatial distributions of the difference in storm track activity (Fig. 6b) and zonal wind (Fig. 6c) are similar to the EOF1 of storm track activity (Fig. 1a) and the EOF2 of zonal wind (Fig. 1b), respectively. Both the PST and AST activities are much stronger in SP than WP, and the difference between the two periods over the North Pacific and North Atlantic is significant at the 95% confidence level. In particular, the intensification of the AST and its downstream extension is noteworthy in difference between two periods. These results agree well with previous work on link between NAO/PNA and storm track activity (Pinto et al. 2011). During the period of 1973–1994 (negative PNA and positive NAO phases), which is nearly coincident with the SP, positive anomalies of storm track activity in North Atlantic and its downstream extension were detected. In addition, a strong link between the circulation over the North Pacific and North Atlantic during the period of 1973–1994 was found (Honda et al. 2001).

For the activity of the two storm tracks, latitudinal and longitudinal locations of the maximum amplitude were unchanged. However, a significant difference of jet configuration is found over the North Pacific and North Atlantic sectors. The maximum change in jet intensity is found downstream of the jet core, i.e. in the storm track core, and the increase of the Atlantic jet intensity is more notable. The northward shift of the Atlantic jet is distinct in Fig. 6c. It has been suggested that variability of the Atlantic jet is closely related to NAO and East Atlantic pattern (Woollings et al. 2010).

In order to see whether the storm track activity exhibits a similar interdecadal shift at other vertical levels, we examine the difference of storm track intensity between SP and WP using the vertical-longitude cross section as shown in Fig. 7. Since the storm track activity is measured in terms of the RMS of the synoptic component of the geopotential height, the maximum activity is seen at the upper levels, particularly at 300-hPa. The strength of the AST activity during NDJFM is larger than the PST at all levels; this may be attributable to the midwinter minimum of the PST activity. The vertical structure of storm track intensity is unchanged from WP (not shown) to SP and the difference between the two periods is significant at all levels, implying that the interdecadal strengthening trend of storm track activity occurs simultaneously at all vertical levels. It has also been found that the storm track activity at the mid and upper levels significantly increased over China, i.e., west of 120°E.

4.2 Change in mean temperature and surface heat flux

In order to causes of the interdecadal change in storm track activity, we investigate changes in mean temperature because baroclinic eddy activity is related to the meridional temperature gradient (Lindzen and Farrell 1980). Since the storm track activity is closely related to the low-level Eady growth rate (e.g. Hoskins and Valdes 1990; Nakamura and

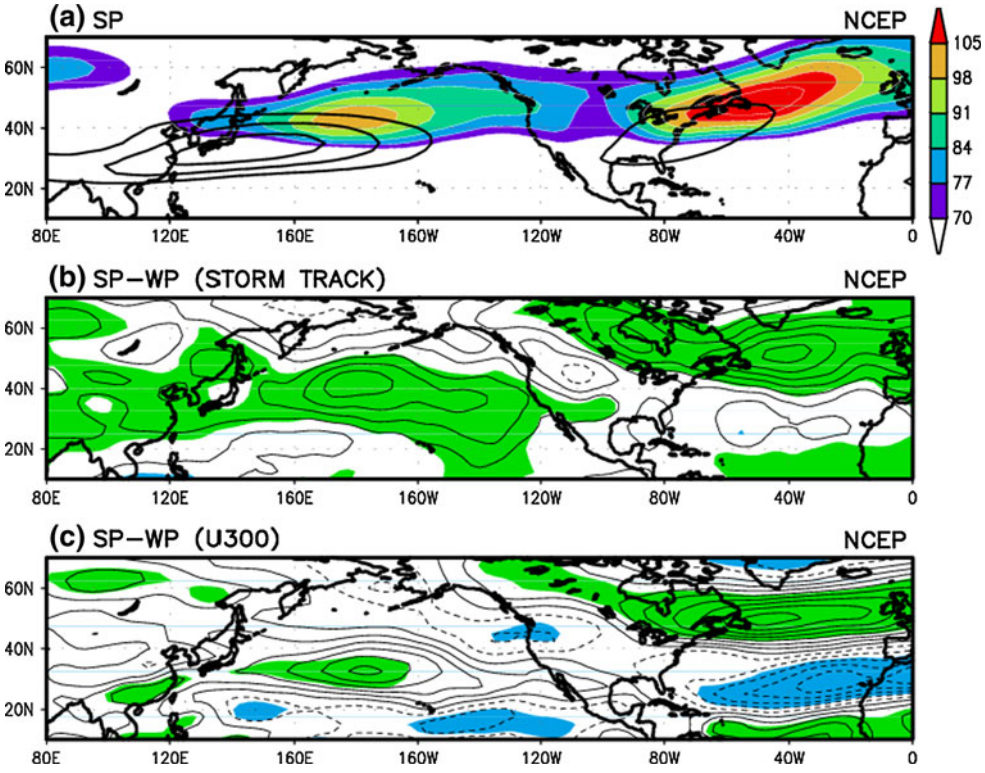

Fig. 6 Root-mean-square of the 2–8 day band-pass filtered 300-hPa geopotential height (storm track activity) (m) (*shadings*) and the corresponding time mean zonal wind (m s^{-1}) (contours) averaged from November to March during the **a** SP (1975/1976–1994/1995). Difference of **b** 300-hPa storm track activity, and **c** 300-hPa zonal wind between the SP and WP. *Shaded areas* in **b** and **c** represent the values significant at the 95% confidence level. The contour level of zonal wind in **a** is 30, 40, and 50 m s^{-1}. The contour intervals are 3 m in **b** and 1 m s^{-1} in **c**, and *dashed lines* indicate negative

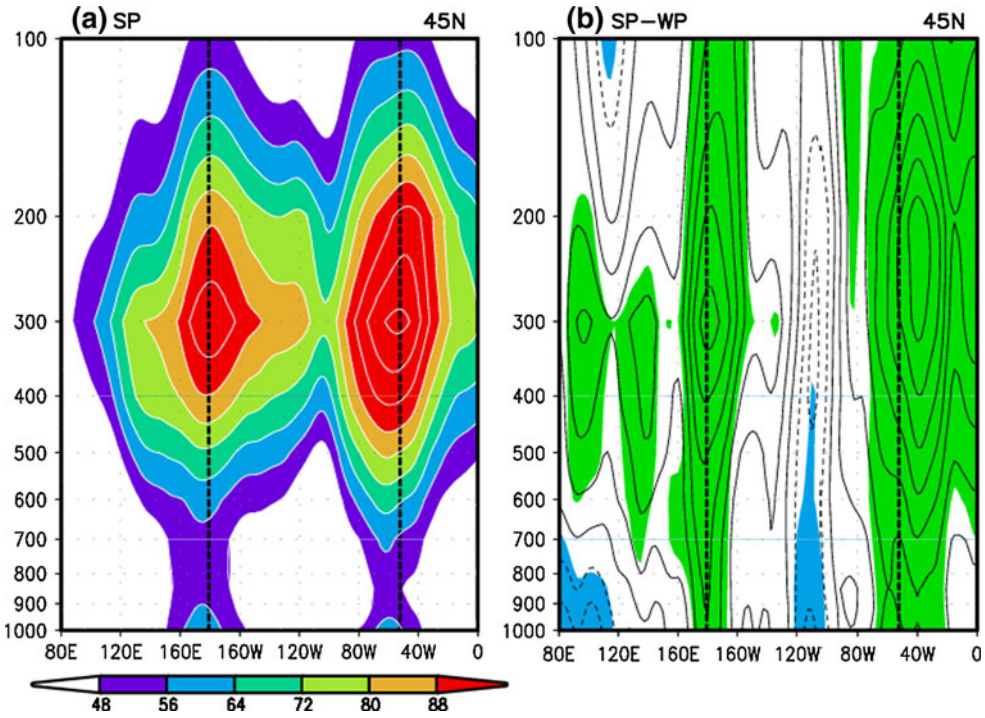

Fig. 7 Vertical-longitude cross sections of the storm track activity (m) along 45°N in **a** SP and **b** its difference between the SP and WP. *Shadings* in **b** represent the values significant at the 95% confidence level and contour interval in **b** is 2 m. The *thick dotted lines* indicate the axis of maximum storm track activity in SP

Shimpo 2004; Penny et al. 2010), difference in temperature between SP and WP at 925-hPa, 850-hPa, and 700-hPa were examined (Fig. 8). It is noted that mean temperature at low-levels significantly increased to the south and decreased to the north of about 35°N (50°N) in the Pacific (Atlantic). Thus, the latitudinal gradient of the mean temperature is enhanced in those zones (i.e., storm track regions) in SP. This suggests that the enhanced meridional thermal gradient can be responsible for the increase of storm track activity in SP.

Furthermore, sensible and latent heat fluxes in the ocean surface play an important role in the energy balance

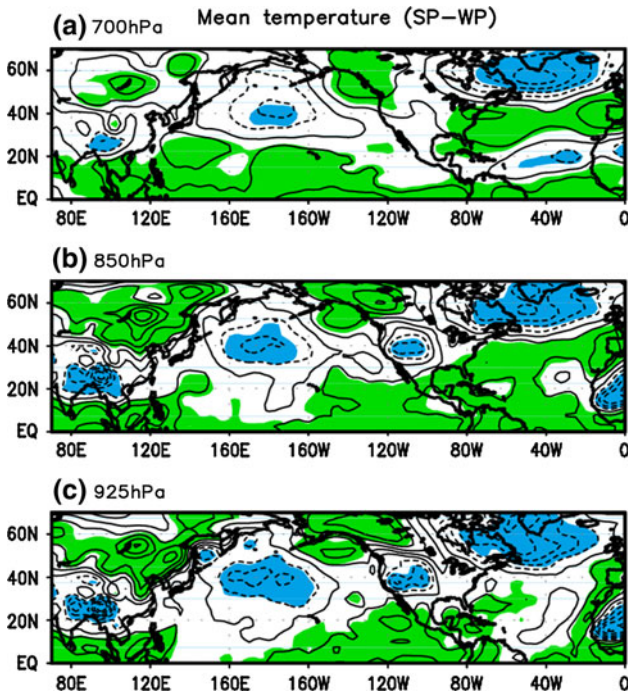

Fig. 8 Difference of mean temperature (K) during NDJFM between SP and WP at **a** 700-hPa, **b** 850-hPa, and **c** 925-hPa. *Shaded areas* represent the values significant at the 95% confidence level. The contour interval is 0.4 K and *dashed lines* indicate negative

between the ocean and atmosphere. The differential heat supply across the oceanic frontal zones can effectively maintain near-surface baroclinicity, and thus help the development of storm track activity (Nonaka et al. 2009; Taguchi et al. 2009; Sampe et al. 2010). Moreover, latent heat fluxes can be important factors in relation to the destabilizing effect of convective heating (Wang and Barcilon 1986). Therefore, the interdecadal change in surface sensible and latent heat fluxes can be one of the possible sources that induce the interdecadal shift of the storm track activity.

Figure 9 shows the surface sensible and latent heat fluxes in SP and the difference between SP and WP using NCEP-1 and ECMWF ERA-40. A positive flux represents a transfer of heat from the ocean to the atmosphere. Large sensible heat flux is evident along the Kuroshio Current in the western North Pacific and over the Gulf Stream in the Atlantic. Although the difference of sensible heat flux over the continental region obtained from NCEP-1 is dissimilar to that from ECMWF ERA-40, the flux over the North Pacific and North Atlantic is similar as well as significant. This increase of sensible heat flux can enhance the baroclinic wave growth over the storm track regions in SP. Large latent heat flux is also found over the Kuroshio Current and Gulf Stream regions (Fig. 9d). A significant difference due to the increase of latent heat flux in SP is seen over the North Pacific and the North Atlantic in the results from both of the reanalysis data sets although the region of significant difference in the North Atlantic is relatively small in the results from NCEP-1 (Fig. 9e) compared to that from ECMWF ERA-40 (Fig. 9f). Tomita and Kubota (2005) also showed the increase in latent heat flux over Kuroshio and Kuroshio/Oyashio extension region due to the increase in SST during the 1990's. The significant increases in surface heat fluxes could be responsible for the reduction of the lower tropospheric static stability and baroclinic wave development in the two storm track regions. On the other side, strong eddy activities can enhance surface sensible and latent heat fluxes. We will also discuss eddy feedback to mean field in the next subsection.

4.3 Change in mean-eddy interaction

Given the fact that the combined effect of poleward and upward heat fluxes and the horizontal momentum plays an important role on the circulation of the atmosphere (Hare and James 2001), we investigate the interdecadal shift in mean flow-eddy interaction by analyzing barotropic and baroclinic energetics. The barotropic and baroclinic energy conversion from ERA-40 is comparable to that from NCEP-1, thus we just present energy conversion from NCEP-1.

4.3.1 Barotropic diagnostics

The barotropic energy conversion between the mean flow and transient eddies in SP and WP is examined in order to determine whether barotropic energetics is associated with the interdecadal shift of storm track activity. Figure 10a and d show the kinetic energy conversion from time-mean flow to eddies at 500-hPa during SP and the difference between SP and WP, derived from the deformation vector (D-vector) of the mean flow and the eddy vector (E-vector). The zonal wind at 300-hPa is superimposed using NCEP-1. The regions where the eddies obtain the kinetic energy from the mean flow (positive shading) is unchanged from WP (not shown) to SP. Transient eddies obtain kinetic energy north of the Pacific jet core and at the Atlantic jet entrance region, which corresponds to the storm track initiation regions (Lee et al. 2011). Over North America, the region where kinetic energy is transferred into eddies from the mean flow slightly expanded to the northeast and eddies acquired much more kinetic energy in SP. Thus the difference between the two periods is significant over the genesis region of the AST, indicating the contribution of barotropic energetics to the interdecadal shift of AST activity. The barotropic decay (mean field gets energy from eddies) is also enhanced, particularly over the North Atlantic. However, it is noted that the change in positive

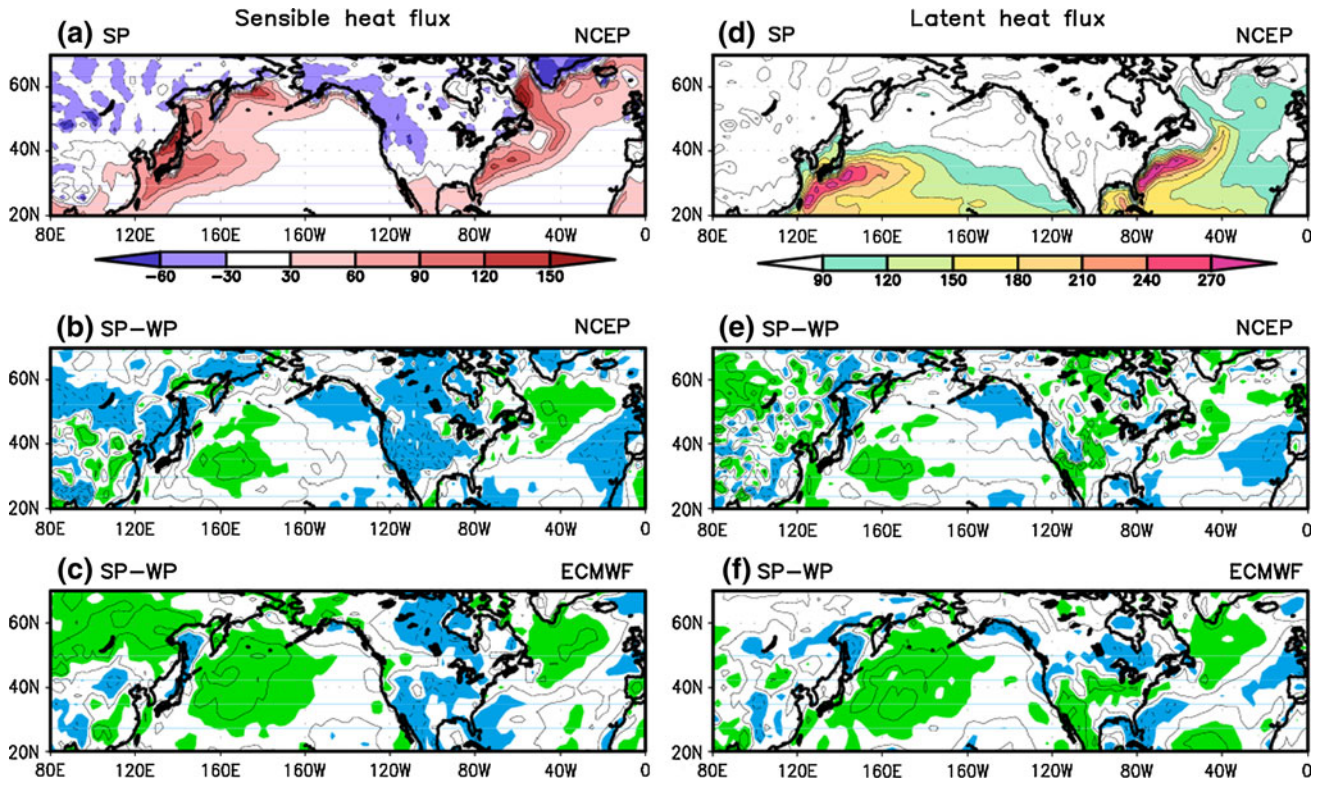

Fig. 9 Sensible heat flux (W m^{-2}) in **a** SP, the flux difference between the SP and WP obtained from **b** NCEP-1, and **c** ECMWF ERA-40. Latent heat flux (W m^{-2}) in **d** SP, the flux difference between the SP and WP obtained from **e** NCEP-1, and **f** ECMWF ERA-40. *Shaded areas* in **b**, **c**, **e** and **f** represent the values significant at the 95% confidence level. The contour intervals are 4 W m^{-2} in **b**, **c**, **e** and **f** and *dashed lines* indicate negative

barotropic energy conversion is insignificant over the North Pacific, suggesting that barotropic energy conversion cannot significantly contribute to the interdecadal strengthening trend of the PST activity. On the contrary, the enhanced barotropic decaying over the eastern North Pacific may enhance the eddy-driven jet and lead to eastward shift of jet maximum shown in Fig. 6c.

4.3.2 Baroclinic diagnostics

The poleward and upward motion of warm air can produce the energy source for the baroclinic wave development (Chang et al. 2002). Therefore, a comparison of baroclinic energy conversion between the two periods is carried out. Figure 10b and e describe the energy conversion from mean available potential energy to eddy available potential energy at 500-hPa during NDJFM in the SP and the difference between SP and WP, which is related to the horizontal eddy heat flux and mean temperature gradient. In particular, meridional temperature gradient is directly linked to the Eady growth rate (Lindzen and Farrell 1980) as a measure of baroclinicity. Compared to the barotropic energetics, the energy conversion from the mean available potential energy to the eddy available potential energy is relatively high. Moreover, the maximum energy conversion occurs upstream of the two storm track regions. Over the North Pacific and North Atlantic sectors, the energy conversion from the mean available potential energy to the eddy available potential energy is significantly increased from WP to SP, consequently, this is indicative of the close relationship with the interdecadal shift of storm track activity. In particular, the pattern of increase in baroclinic energy conversion in the North Atlantic is comparable to that of the AST activity. As aforementioned, the AST activity is closely related to the PNA and NAO. During the negative PNA and positive NAO phases, an advection of moist and warm air related to the latent heat from the Gulf of Mexico and that of cold and dry air from Arctic can lead to the strong storm track activity in the North Atlantic (Pinto et al. 2011). They also noted that this advection contributes to increase of baroclinicity which modulates the growth condition for baroclinic waves in the North Atlantic. This mechanism agrees with the sources for intensification of storm track activity (i.e., surface heat fluxes and temperature gradient) discussed in Sect. 4.2.

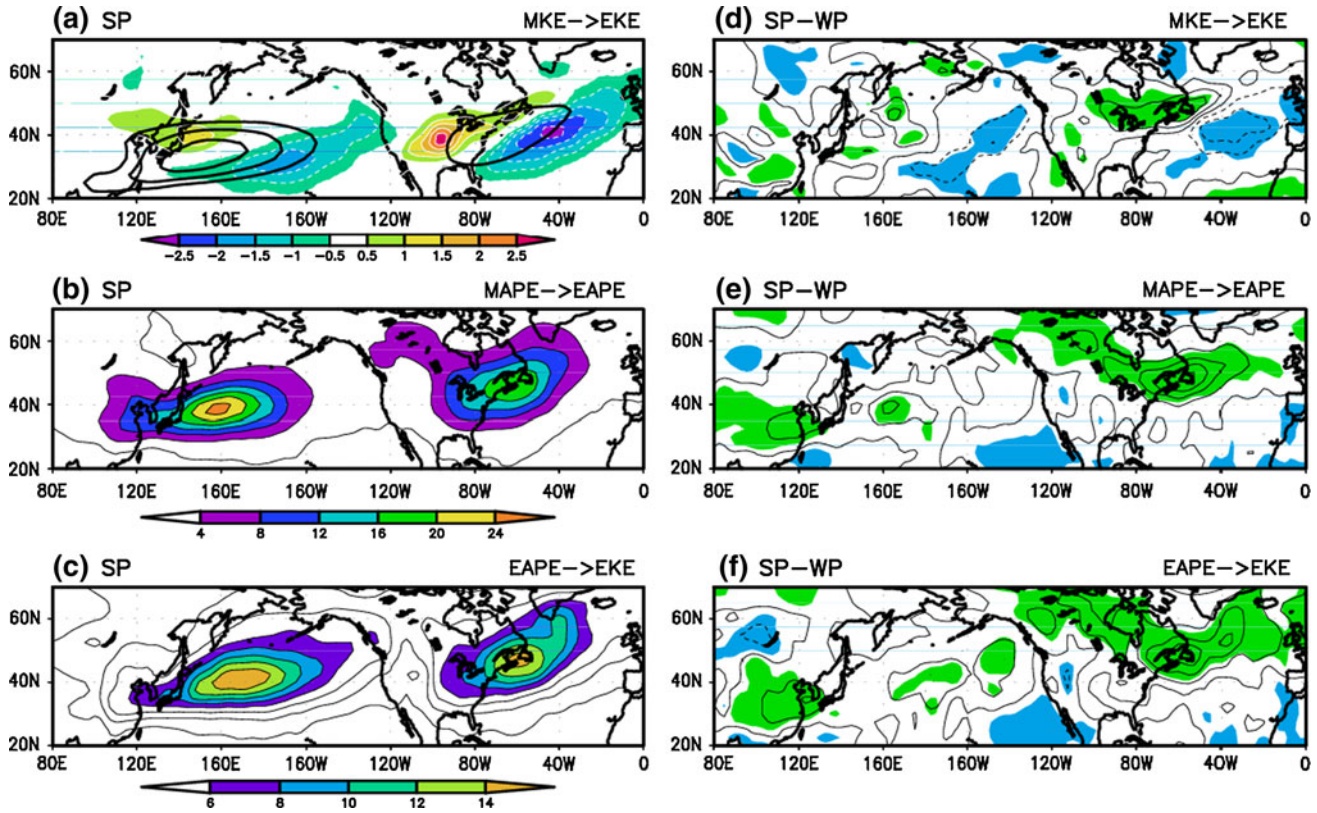

Fig. 10 **a** Energy conversion (W m^{-2}) (*shading*) from mean kinetic energy to eddy kinetic energy (MKE → EKE) at 500-hPa in SP and **d** its difference (contour interval: 0.4 W m^{-2}) between the SP and WP. **b** Energy conversion (W m^{-2}) from mean available potential energy to eddy available potential energy (MAPE → EAPE) at 500-hPa in SP and **e** its difference (contour interval: 2.0 W m^{-2}) between the SP and WP. **c** Energy conversion (W m^{-2}) from eddy available potential energy to eddy kinetic energy (EAPE → EKE) at 500-hPa in SP and **f** its difference (contour interval: 1.0 W m^{-2}) between the SP and WP. The contour in **a** indicates zonal wind at 500-hPa (15, 20, 25, 30 m s^{-1}). *Shaded areas* in **d**–**f** represent the values significant at the 95% confidence level. *Dashed lines* in **d**–**f** indicate negative

Meanwhile, the relatively weak increase of baroclinic energy conversion in the North Pacific may be related to the insignificant increment of the PST intensity during midwinter (Fig. 4c). It is noted that the maximum amplitude of PST activity (180°) is located further downstream of the position of maximum baroclinic energy conversion (160°E) compared to that in the North Atlantic. In addition, the increase of baroclinic energy conversion is also significant over eastern China and Korea.

Figure 10c exhibits the energy conversion between the eddy available potential energy and eddy kinetic energy induced by the upward eddy heat flux. This energy conversion shows an increasing pattern (Fig. 10f) similar to the energy conversion from the mean available potential energy to the eddy available potential energy, particularly over the North Atlantic. The results from ECMWF ERA-40 show very weak increase of this energy conversion in the North Pacific (not shown).

Furthermore, the changes of baroclinic energetics in the vertical structure are examined using the vertical-longitude cross section (Fig. 11). The latitudinal band [32.5°–57.5°N] showing large baroclinic energy conversion in the North Pacific and North Atlantic is averaged. Over the PST and AST regions, as in the storm track intensity, the baroclinic energetics significantly increased from WP to SP at all vertical levels. The significant increase of energy conversion from the mean available potential energy to the eddy available potential energy is found in the upstream of the PST, i.e., to the west of 180°, at the upper level. In the North Atlantic, energy conversion from the mean available potential energy to the eddy available potential energy significantly increased from surface to the 300-hPa (Fig. 11a). The conversion from eddy available potential to eddy kinetic energy and its difference are the greatest at mid-level along the axis of maximum storm track activity, particularly in the North Atlantic (Fig. 11b). This indicates that the increase of baroclinic energy conversion over the North Pacific and North Atlantic is related to the enhancement of storm track activity in SP.

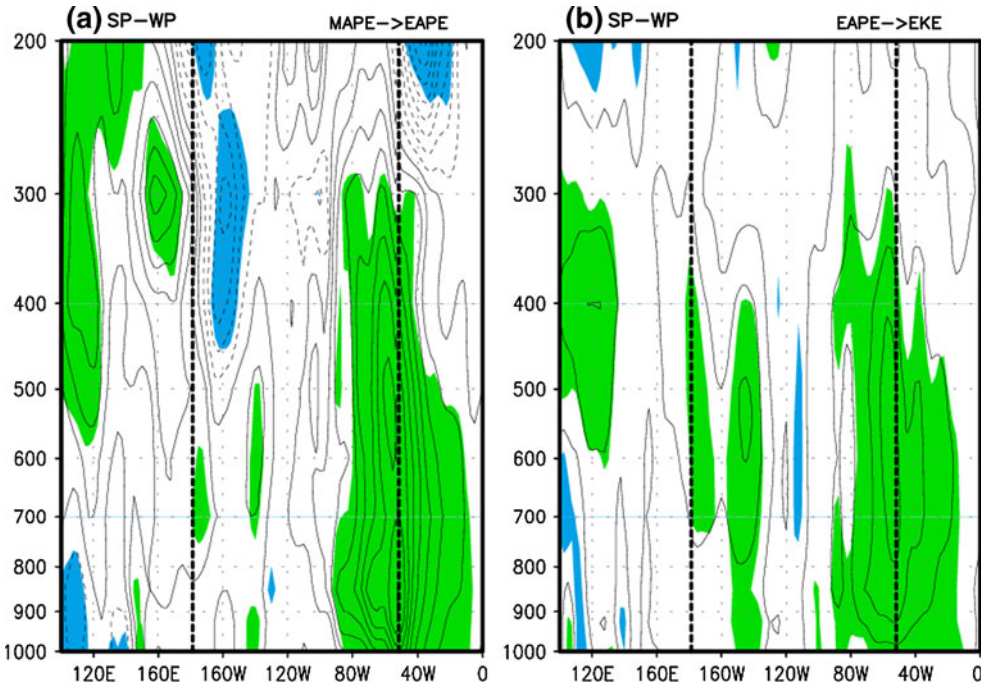

Fig. 11 Vertical-longitude cross section for difference of **a** energy conversion from mean available potential energy to eddy available potential energy and **b** energy conversion from eddy available potential energy to eddy kinetic energy along 32.5°–57.5°N between the SP and WP. *Shadings* represent the values significant at the 95% confidence level and the *thick dotted lines* indicate the axis of maximum storm track activity

4.3.3 Changes in eddy feedback to mean field

This subsection investigates whether the mid-1970s' shift in storm track activity, in turn, played a certain role in the changes in mean field. Figure 12 shows the 500-hPa geopotential height and 850-hPa temperature tendency. The transient eddies basically tend to enhance (reduce) north–south gradient of the height (temperature) field shown in Fig. 12a and c and the feedback was significantly enhanced in both geopotential height and temperature field after the mid-1970s (Fig. 12b, d). The height tendency is consistent with northward (poleward) movement of the jets, while the temperature tendency implies a flattening of the meridional gradient. It is noted that changes in the storm track activity over the North Pacific and North Atlantic helped to reinforce and maintain the changes in the middle-to-upper tropospheric circulation but to interfere with changes in the low-tropospheric temperature field, similar to the result of Trenberth and Hurrell (1994). In summary, the enhanced storm track activity after the mid-1970s played an important role to reinforce and maintain the mean changes in middle-to-upper tropospheric circulation but acted to

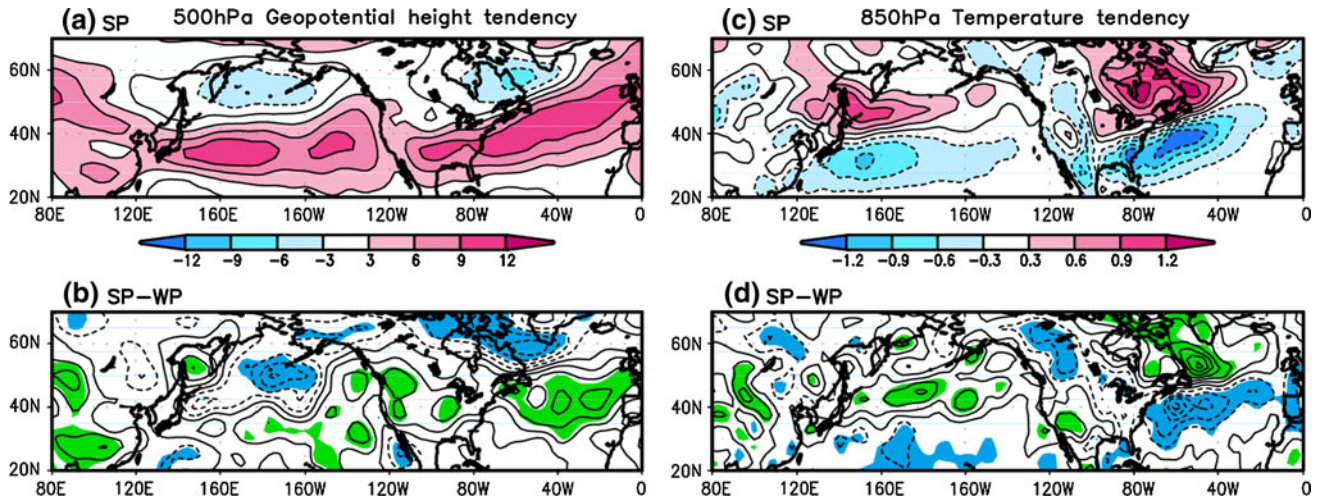

Fig. 12 **a** 500-hPa geopotential height tendency (m day^{-1}) and **b** 850-hPa temperature tendency (°C day^{-1}) in SP. Difference of **b** 500-hPa geopotential height tendency (m day^{-1}) and **d** 850-hPa temperature tendency (°C day^{-1}) between SP and WP. *Shaded areas* in **b** and **d** represent the values significant at the 95% confidence level. The contour intervals are 1 m day^{-1} in **b** and 0.1°C day^{-1} in **d**, and *dashed lines* indicate negative

interfere with changes in the low-tropospheric temperature field.

5 Summary and discussion

The interdecadal changes in storm track activity and its associated mean flow-eddy interaction are investigated in terms of barotropic and baroclinic energetics and eddy feedback to mean field using the NCEP-1 and ECMWF ERA-40 reanalysis data. The EOF analysis of RMS of the band-pass filtered 300-hPa geopotential height for 62 years reveals that the PST and AST activity during the cool season (NDJFM) in the NH have increased significantly around the early-to-mid 1970s. This result was derived not only from the NCEP-1 but also from the ECMWF ERA-40. The EOF1 of global storm track activity is significantly related to the EOF2 of zonal wind at 300-hPa. The PST activity is closely linked that in the extratropics of NH during 62 years whereas the AST activity has insignificant relationship with global storm track activity from 1972–1992 to 1983–2003. It is interestingly to note that decoupling of significant connection of the PST and AST activity is found since the early 1980s. In particular, the interdecadal transitions of PST and AST show notable differences in subseasonal time scales. The PST activity in midwinter shows decadal change from weak regime during the early 1980s to strong regime during the late 1980s and the intensity in early spring increased during recent decade compared to that in SP. However, the AST intensity in midwinter weakened in the latest decade.

There is interdecadal change in relationship between the storm track activity and climate indices. The linkage with PDO and NAO shows a similar change from 1960s to 1990s. The storm track activity was highly correlated with the PDO and NAO during 1960–1980, whereas these significant relationships have considerably weakened since the early 1980s. A strong linkage with the PNA index is found during 1970–1980. However, the global storm track activity has no significant relationship with the AO for 60 years. The relationship between the storm track activity and Niño 3.4 exhibits opposite interdecadal change to that with PDO or NAO, from a weak correlation regime during 1960–1980 to a strong correlation regime during 1980–2000. The causes for this change in relationship between PST and AST activity and storm track activity and climate indices would be an interesting area for future research.

We further examine changes in mean temperature and surface heat fluxes to find sources for the enhancement of storm track activity after the mid-1970s. The interdecadal shift of storm track activity can be attributed to a significant increase of meridional temperature gradient related to baroclinicity over the North Pacific and North Atlantic. It is also found that an increase of surface heat fluxes in the storm track regions. Although the increased storm track activity is associated with an increase of surface heat fluxes, the increase of surface heat fluxes can be a result of enhanced storm activity. The feedback process between storm track activity and surface heat fluxes require further studies with climate models.

In order to better understand the mid-1970s' shift in storm track activity and mean flow-eddy interaction, an analysis of local barotropic and baroclinic energetics and eddy feedback to mean field is also made. The role of barotropic energy conversion on the interdecadal shift of PST is insignificant while the enhanced kinetic energy conversion from the mean flow to the eddies over North America (upstream of the maximum AST activity) is related to intensification of the AST activity. Meanwhile, baroclinic energetics is closely associated with the intensification of storm track activity. It is noted that baroclinic energy conversion related to the eddy heat flux and mean meridional temperature gradient over the North Pacific and North Atlantic is significantly associated with the strengthening trend of the storm track activity. In addition, changes in eddy feedback to mean field indicates that enhanced storm track activity after the mid-1970s plays an important role to reinforce and maintain the mean changes in middle-to-upper tropospheric circulation but acts to interfere with changes in the low-tropospheric temperature field.

In this study, the interdecadal variability of storm tracks and mean flow-eddy interaction during the boreal cool season is considered, focusing on the relationship with the local energetics and eddy feedback. Given different subseasonal variation of the two storm tracks, the interdecadal change of the transient eddies in midwinter, fall/spring and monthly mean and its associated local energetics may be different from that of the NDJFM mean. Therefore, more detailed analyses of these issues need to be made in the future. Moreover, other processes such as changes in land surface conditions related to the changes in snow cover or blocking are potential candidates to help explain the intensification of the storm track activity after mid-1970s. Chen and Yoon (2002) suggested that the North Pacific blocking activity shows a noticeable interdecadal change over the past four decades. It was found that the blocking days increased and blocking highs shifted eastward. More work will be done to ascertain the roles of background circulation and state on the interdecadal variability of storm track activity.

Acknowledgments This work was supported by the Global Research Laboratory (GRL) Program from the Ministry of Education, Science and Technology (MEST), Korea. J.-Y. Lee and B. Wang acknowledge support from the Korean Meteorological Administration Research and Development Program under Grant RACS 2010–2017

and from International Pacific Research Center, which is in part supported by JAMSTEC, NOAA, and NASA. This is SOEST publication number 8483 and IPRC publication number 817.

Appendix

Barotropic and baroclinic energy conversion

The barotropic energy conversion (BTEC) can be expressed by the inner product of the D-vector of the basic flow and the E-vector of the transient parts (Cai et al. 2007). The D-vector defined as $\vec{D} = \left(\frac{\partial \bar{u}}{\partial x} - \frac{\partial \bar{v}}{\partial y}, \frac{\partial \bar{v}}{\partial x} + \frac{\partial \bar{u}}{\partial y}\right)$ consists of the stretching and shearing deformations. The E-vector defined as $\vec{E} = \left(\frac{1}{2}\left(\overline{v'^2} - \overline{u'^2}\right), -\overline{u'v'}\right)$ is a measure of the local shape and horizontal orientation of eddies (Cai and Mak 1990).

$$\mathrm{BTEC} = \frac{p_0}{g}\left\{\frac{1}{2}\left(\overline{v'^2} - \overline{u'^2}\right)\left(\frac{\partial \bar{u}}{\partial x} - \frac{\partial \bar{v}}{\partial y}\right) + \left(-\overline{u'v'}\right)\left(\frac{\partial \bar{v}}{\partial x} + \frac{\partial \bar{u}}{\partial y}\right)\right\}$$

where, g is the acceleration of gravity and p_0 is 1,000 hPa. The overbar and prime represent the climatological mean and transient parts, respectively.

The baroclinic generation from mean available potential energy to eddy available potential energy (BCEC I) is roughly proportional to the poleward eddy heat flux multiplied by the meridional temperature gradient (Dole and Black 1990; Cai et al. 2007).

$$C_1 = \left(\frac{p_0}{p}\right)^{C_V/C_P}\frac{R}{g}$$

$$C_2 = C_1\left(\frac{p_0}{p}\right)^{R/C_P} \Big/ \left(-\frac{d\Theta}{dp}\right)$$

$$\mathrm{BCEC\ I} = -C_2\left(\overline{u'T'}\frac{\partial \bar{T}}{\partial x} + \overline{v'T'}\frac{\partial \bar{T}}{\partial y}\right)$$

where, R is the gas constant for dry air and C_P (C_V) is the specific heat of dry air at the constant pressure (volume). Θ indicates potential temperature.

The energy conversion between eddy available potential energy and eddy kinetic energy (BCEC II) can be expressed by upward heat flux (Dole and Black 1990; Cai et al. 2007)

$$\mathrm{BCEC\ II} = -C_1\left(\overline{\omega'T'}\right).$$

Eddy feedback

The geopotential height and temperature tendency from eddy feedback are calculated by vorticity and heat flux convergences of the transient eddies according to Cai et al. (2007)

$$\frac{\partial h}{\partial t} = \nabla^{-2}\left[-\frac{f_0}{g}\overline{\nabla \cdot (\vec{V}'\zeta')}\right]$$

$$\frac{\partial T}{\partial t} = -\overline{\nabla \cdot (\vec{V}'T')}.$$

Lepage test statistic

The Lepage test statistic is a useful tool for detecting significant changes between two samples (Yonetani and McCabe 1994). Using the Lepage test, we can detect changes in the mean and in the variance of variable through time. The Lepage test statistic is calculated as follow.

$$\text{Lepage test statistic} = \frac{\left[\sum_{i=1}^{N} i \cdot u_i - \frac{1}{2}n_1(N+1)\right]^2}{\frac{1}{12}n_1 n_2 (N+1)} + \frac{\left[\sum_{i=1}^{n_1} i \cdot u_i + \sum_{i=n+1}^{N}(N-i+1)u_i - \frac{1}{4}n_1(N+2)\right]^2}{\frac{n_1 n_2 (N-2)(N+2)}{48(N-1)}}$$

where, n_1 and n_2 are sample sizes of samples a and b respectively. The N is sum of n_1 and n_2. The $u_i = 1$ when the ith record in a combined sample of ranked values of samples a and b belongs to the sample a, and $u_i = 0$ when it belongs to the sample b. If the Lepage test statistic is greater than 5.99 (9.21), the change between two samples is significant at a 95% (99%) confidence level. Details of Lepage test are described in Yonetani and McCabe (1994).

References

Baldwin MP, Dunkerton TJ (2001) Stratospheric harbingers of anomalous weather regimes. Science 244:581–584

Blackmon ML (1976) A climatological spectral study of the 500 mb geopotential height of the northern hemisphere. J Atmos Sci 33:1607–1623

Blackmon ML, Wallace JM, Lau NC, Mullen SL (1977) An observational study of the northern hemisphere wintertime circulation. J Atmos Sci 34:1040–1053

Cai M, Mak M (1990) On the basic dynamics of regional cyclogenesis. J Atmos Sci 47:1417–1442

Cai M, Yang S, Van den Dool HM, Kousky VE (2007) Dynamical implications of the orientation of atmospheric eddies: a local energetics perspective. Tellus 59A:127–140

Castanheira JM, Graf HF (2003) North Pacific-North Atlantic relationships under stratospheric control? J Geophys Res 108:4036. doi:10.1029/2002JD002754

Chang EKM (2004) Are the northern hemisphere winter storm tracks significantly correlated? J Clim 17:4230–4244

Chang EKM, Fu Y (2002) Interdecadal variations in northern hemisphere winter storm track intensity. J Clim 15:642–658

Chang EKM, Fu Y (2003) Using mean flow change as a proxy to infer interdecadal storm track variability. J Clim 16:2178–2196

Chang EKM, Lee S, Swanson KL (2002) Storm track dynamics. J Clim 15:2163–2183

Chen TC, Yoon JH (2002) Interdecadal variation of the North Pacific wintertime blocking. Mon Weather Rev 130:3136–3143

Dole RM, Black RX (1990) Life cycles of persistent anomalies. Part II: the development of persistent negative height anomalies over the North Pacific Ocean. Mon Weather Rev 118:824–846

Eichler T, Higgins W (2006) Climatology and ENSO-related variability of North American extratropical cyclone activity. J Clim 19:2076–2093

Hare SHE, James IN (2001) Baroclinic developments in jet entrances and exits. I: linear normal modes. Q J R Meteorol Soc 127:1293–1303

Harnik N, Chang EKM (2003) Storm track variations as seen in radiosonde observations and reanalysis data. J Clim 16:480–495

Honda M, Nakamura H (2001) Interannual seesaw between the Aleutian and Icelandic lows. Part II: its significance in the interannual variability over the wintertime northern hemisphere. J Clim 14:4512–4529

Honda M, Nakamura H, Ukita J, Kousaka I, Takeuchi K (2001) Interannual seesaw between the Aleutian and Icelandic lows. Part I: seasonal dependence and life cycle. J Clim 14:1029–1042

Honda M, Yamane S, Nakamura H (2005) Impacts of the Aleutian-Icelandic low seesaw on surface climate during the twentieth century. J Clim 18:2793–2802

Hoskins BJ, Valdes PJ (1990) On the existence of storm tracks. J Atmos Sci 47:1854–1864

Jin FF (2010) Eddy-Induced instability for low-frequency variability. J Atmos Sci 67:1947–1964

Kalnay E et al (1996) The NCEP/NCAR 40-Year reanalysis project. Bull Am Meteor Soc 77:437–471

Kug JS, Jin FF, Par JH, Ren HL, Kang IS (2010) A general rule for synoptic-eddy feedback onto low-frequency flow. Clim Dyn 35:1011–1026

Latif M, Barnett TP (1994) Causes of decadal climate variability over the North Pacific and North America sector. Science 266:634–637

Lau NC (1988) Variability of the observed midlatitude storm tracks in relation to low-frequency changes in the circulation patterns. J Atmos Sci 45:2718–2743

Lee S (2000) Barotropic effects on atmospheric storm tracks. J Atmos Sci 57:1420–1435

Lee SS, Lee JY, Wang B, Jin FF, Lee WJ, Ha KJ (2011) A comparison of climatological subseasonal variations in the wintertime storm track activity between the North Pacific and Atlantic: local energetics and moisture effect. Clim Dyn. Published online doi:10.1007/s00382-011-1027-z

Lindzen RS, Farrell BJ (1980) A simple approximate result for the maximum growth rate of baroclinic instabilities. J Atmos Sci 37:1648–1654

Mak M, Deng Y (2007) Diagnostic and dynamical analyses of two outstanding aspects of storm tracks. Dyn Atmos Oceans 43:80–99

Nakamura H (1992) Midwinter suppression of baroclinic wave activity in the Pacific. J Atmos Sci 49:1629–1642

Nakamura H, Shimpo A (2004) Seasonal variations in the southern hemisphere storm tracks and jet streams as revealed in a reanalysis dataset. J Clim 17:1828–1844

Nakamura H, Izumi T, Sampe T (2002) Interannual and decadal modulations recently observed in the Pacific storm track activity and East Asian winter monsoon. J Clim 15:1855–1874

Nie J, Wang P, Yang W, Tan B (2008) Northern hemisphere storm tracks in strong AO anomaly winters. Atmos Sci Let 9:153–159

Nonaka M, Nakamura H, Taguchi B, Komori N, Yoshida-Kuwano A, Takaya K (2009) Air-sea heat exchanges characteristic to a prominent midlatitude oceanic front in the South Indian Ocean as simulated in a high-resolution coupled GCM. J Clim 22:6515–6535

Orsolini YJ, Kvamstø NG, Kindem IT, Honda M, Nakamura H (2008) Influence of the Aleutian-Icelandic low seesaw and ENSO onto the Stratosphere in ensemble winter hindcasts. J Meteorol Soc Jpn 86:817–825

Penny S, Gerard HR, David SB (2010) The source of the midwinter suppression in storminess over the North Pacific. J Clim 23:634–648

Pinto JG, Reyers M, Ulbrich U (2011) The variable link between PNA and NAO in observations and in multi-century CGCM simulations. Clim Dyn 36:337–354

Raible CC, Luksch U, Fraedrich K, Voss R (2001) North Atlantic decadal regimes in a coupled GCM simulation. Clim Dyn 18:321–330

Rivière G, Orlanski I (2007) Characteristics of the Atlantic storm-track eddy activity and its relation with the North Atlantic Oscillation. J Atmos Sci 64:241–266

Sampe T, Nakamura H, Goto A, Ohfuchi W (2010) Significance of a midlatitude SST frontal zone in the formation of a storm track and an eddy-driven westerly jet. J Clim 23:1793–1814

Straus DM, Shukla J (1997) Variations of midlatitude transient dynamics associated with ENSO. J Atmos Sci 54:777–790

Taguchi B, Nakamura H, Nonaka M, Xie SP (2009) Influences of the Kuroshio/Oyashio extensions on air–sea heat exchanges and storm-track activity as revealed in regional atmospheric model simulations for the 2003/04 cold season. J Clim 22:6536–6560

Tomita H, Kubota M (2005) Increase in turbulent heat flux during the 1990s over the Kuroshio/Oyashio extension region. Geophys Res Lett 32:L09705. doi:10.1029/2004GL022075

Trenberth KE (1990) Recent observed interdecadal climate changes in the northern hemisphere. Bull Am Meteor Soc 71:988–993

Trenberth KE, Hurrell JW (1994) Decadal atmosphere-ocean variations in the Pacific. Clim Dyn 9:303–319

Uppala SM et al (2005) The ERA-40 re-analysis. Q J R Meteorol Soc 131:2961–3012

van Loon H, Rogers JC (1978) The seesaw in winter temperatures between Greenland and Northern Europe. Part I: general description. Mon Weather Rev 106:296–310

Wang B, Barcilon A (1986) Moist stability of a baroclinic zonal flow with conditionally unstable stratification. J Atmos Sci 43:705–719

Woollings T, Hannachi A, Hoskins B (2010) Variability of the North Atlantic eddy-driven jet stream. Q J R Meteorol Soc 136:856–868

Yonetani T, McCabe GJ (1994) Abrupt changes in regional temperature in the conterminous United States. Clim Res 4:12–23

Zhang Y, Held IM (1999) A linear stochastic model of a GCM's midlatitude storm tracks. J Atmos Sci 56:3416–3435

Zhang R, Li G, Fan J, Wu DL, Molina MJ (2007) Intensification of Pacific storm track linked to Asian pollution. Proc Nat Acad Sci 104:5295–5299

Zhu W, Sun Z (1999) Influence of ENSO event on the maintenance of Pacific storm track in the Northern winter. Adv Atmos Sci 16:630–640